Patient-Specific Modelling of Abdominal Aortic Aneurysms: The Influence of Wall Thickness on Predicted Clinical Outcomes

Citation for published version:
Conlisk, N, Geers, A, Mcbride, O, Newby, D & Hoskins, P 2016, 'Patient-Specific Modelling of Abdominal Aortic Aneurysms: The Influence of Wall Thickness on Predicted Clinical Outcomes', *Medical Engineering and Physics*, vol. 38, no. 6. https://doi.org/10.1016/j.medengphy.2016.03.003

Digital Object Identifier (DOI):
10.1016/j.medengphy.2016.03.003

Published In:
Medical Engineering and Physics

Patient-Specific Modelling of Abdominal Aortic Aneurysms: The Influence of Wall Thickness on Predicted Clinical Outcomes.

Noel Conlisk, [1] Arjan J. Geers, [1] Olivia M.B. Mc Bride, [1] David E. Newby, [1, 2] and Peter R. Hoskins, [1]

Running title: Influence of AAA wall thickness.

[1] British Heart Foundation/University of Edinburgh Centre for Cardiovascular Science, Edinburgh, UK

[2]Clinical Research Imaging Centre, The University of Edinburgh, Edinburgh, UK

Correspondence:
Dr. Noel Conlisk
Room E3.24,
The Queen's Medical Research Institute,
47 Little France Crescent,
The University of Edinburgh,
EH16 4TJ, Edinburgh, UK
Phone: (+44) 7775 332506
Email: noel.conlisk@ed.ac.uk

ABSTRACT

Rupture of abdominal aortic aneurysms (AAAs) is linked to aneurysm morphology. This study investigates the influence of patient-specific (PS) AAA wall thickness on predicted clinical outcomes. Eight patients under surveillance for AAAs were selected from the MA^3RS clinical trial based on the complete absence of intraluminal thrombus. Two finite element (FE) models per patient were constructed; the first incorporated variable wall thickness from CT (PS_wall), and the second employed a 1.9mm uniform wall (Uni_wall). Mean PS wall thickness across all patients was 1.77 ± 0.42mm. Peak wall stress (PWS) for PS_wall and Uni_wall models was 0.6761 ± 0.3406N/mm^2 and 0.4905 ± 0.0850N/mm^2 respectively. In 4 out of 8 patients the Uni_wall underestimated stress by as much as 55%; in the remaining cases it overestimated stress by up to 40%. Rupture risk more than doubled in 3 out of 8 patients when PS_wall was considered. Wall thickness influenced the location and magnitude of PWS as well as its correlation with curvature. Furthermore, the volume of the AAA under elevated stress increased significantly in AAAs with higher rupture risk indices. This highlights the sensitivity of standard rupture risk markers to the specific wall thickness strategy employed.

KEYWORDS: Abdominal aortic aneurysms; finite element analysis; patient-specific modelling; patient-specific wall thickness; rupture risk

1. INTRODUCTION

Abdominal aortic aneurysms (AAAs) are typically characterised by a large dilation of the aorta below the renal arteries. Each year over 10,000 deaths in the UK are attributed to rupture of AAAs [1]. Rupture occurs when the stress at any point in the wall exceeds its strength. Surgical repair is typically considered for asymptomatic aneurysms, when the maximum diameter passes 55mm, or the growth rate exceeds 10mm/year [2]. However, intervention also carries a risk (approximately 2.5%) of mortality [1]. Furthermore, ruptured aneurysms with maximum diameters below the 55mm threshold account for 10 - 24% of all cases [3-5], conversely 60% of AAAs above 55mm never rupture [6]. This indicates that maximum diameter criterion alone is not able to discern all cases which require intervention. Several techniques have been suggested to complement the maximum diameter criterion; AAA wall stress predicted using computational models [7-13], AAA growth rate [14, 15], rupture risk indices [16-18], integrity of thrombus [19], geometrical factors (e.g. growth, asymmetry) [20-23].

A number of computational studies [24], have suggested that peak wall stress (PWS) derived from finite element (FE) models has the ability to assess rupture risk more accurately than existing clinical indices. However, the accuracy of such predictions relies on realistic physical representation of the system they are modelling [25]. Ideally a number of physical factors must be known for the individual patient including a clear definition of the aneurysm geometry, its material properties, the manner in which it interacts with other bodily structures, and the internal/external forces acting on the aneurysm. Early computational models often employed straight tubes with symmetrical central dilations or asymmetric bulges to act as aneurysm analogues [21, 22]. Due to the proliferation of high powered desktop computing and advances in three-dimensional imaging techniques, it is now possible to generate highly

accurate virtual reconstructions of patient-specific (PS) aneurysms from medical imaging data [26] acquired using modalities such as computed tomography (CT) and magnetic resonance imaging (MRI). However, one particularly challenging aspect of the reconstruction process for AAAs is accurate determination of the vessel wall.

At present, it is currently not possible to determine the wall-thrombus interface explicitly from CT with existing scanners, though recent developments in multimodal imaging may overcome this issue in the future [27], as a consequence virtually all early computational studies of AAAs have assumed a uniform wall thickness of 1.9mm e.g. [28]. However, from previous studies [29-31] it is known that aortic wall thickness varies considerably from region to region within the same patient, and across different patients. Therefore, the assumption of a uniform wall may not be adequate when attempting to characterise the response of the aneurysm. As such, this is regarded as a serious limitation of current patient-specific modelling studies [32], yet only a handful of studies have attempted to address its effects [7, 9-11, 13, 21, 28, 33-38].

This study aims to assess the importance of patient-specific wall thickness, derived directly from high resolution CT scans, in a small population of aneurysms which lacked thrombus, while also testing the validity of the widely applied uniform wall assumption and its impact on predicted clinical outcomes.

2. METHODS

2.1 Patient selection and imaging

Computed tomography (CT) scans of 350 individual patients undergoing AAA surveillance, were selected from the MA^{3}RS clinical trial database [39] for reconstruction. Patients underwent both magnetic resonance imaging (MRI) and CT scanning as part of the trial. In each instance CT scanning of the aorta was performed from just below the thoracic arch to below the iliac bifurcation (Aquilion One, Toshiba Medical Systems Ltd, UK). The slice thickness was 0.5mm, with a pixel size of 0.625mm.

The majority of AAAs (75%) tend to have thrombus [10], this can cause great difficulty during the reconstruction phase due to the poor contrast between thrombus and adjacent wall structures, as can be seen in the last panel of Fig. 1a. Therefore, to allow reconstruction of wall thickness direct from the CT scan the selection criteria for the current study was based on the total absence of intraluminal thrombus, in such instances only the lumen and wall are visible directly on the CT scan (Fig. 1b), meaning patient-specific wall geometry can be easily extracted using basic segmentation tools.

In this study, the absence of thrombus was verified by a qualified cardiovascular surgeon on MRI scans of each patient. After exclusion only 10 patients remained, of these 10 only 8 patients had a corresponding CT available for reconstruction (7 male and 1 female). All AAAs were infrarenal, with the main sac approximately located between the L4 and L2 vertebrae. The mean patient age was 76 years (64 – 83 years) and the mean maximum diameter from ultrasound was 46mm (36 – 59mm), individual patient details for all 8 patients investigated are presented in Table 1.

2.2 Three-dimensional reconstruction and meshing

Segmentation and reconstruction of each patient-specific AAA was carried out with commercial software (Mimics innovation suite, Materialise, Belgium) and followed the general workflow presented in Fig. 2. The luminal region was segmented automatically using a thresholding approach, and the outer wall was segmented in a semi-automatic manner using a 3D live wires approach with manual correction of the wall contours on certain slices where the outer boundary was ambiguous (e.g. close to the duodenum). Given that there was physically no thrombus in these selected patient, a true patient-specific wall thickness (PS_wall) was then obtained as the difference between the contrast enhanced lumen and the outer wall, without any need for incorporation of complex "black box" wall thickness estimation algorithms. For comparison a uniform wall thickness version (Uni_wall) of each AAA was also reconstructed, this approach involved merely offsetting the luminal surface outward in the radial direction by a fixed distance, 1.9mm [28], thereby creating an aneurysm with a constant uniform wall thickness.

In all cases, for both wall types (PS_wall and Uni_wall), volume preserving smoothing was performed to remove scanning artefacts and tetrahedral volume meshing operations were performed in 3-matic (Materialise). It is important to note that, for each patient both model variations (PS_wall and Uni_wall) retained identical luminal surfaces, furthermore, both were identically clipped to allow comparison of the exact same regions of interest. Final FE meshes were exported to Abaqus (Abaqus 6.10-1, Dassault Systemes, Simulia, Providence, RI, USA) for analysis.

144 *2.3 Material definition*

145 In the present study the aortic wall was modelled as non-linear, hyperelastic, and
146 incompressible, with the same properties used to represent the behaviour of both uniform and
147 patient-specific walls. Determination of patient-specific aortic wall mechanical properties is
148 essential in accurately assessing the rupture risk of any AAA; however, at present this is not
149 possible by non-invasive means. Through the experimental data of 69 AAA specimens,
150 Raghavan and Vorp [28] characterised the diseased aortic wall by means of a 2nd order
151 reduced polynomial strain energy density function $W = \alpha(IB - 3) + \beta(IB - 3)^2$, where
152 W is the strain energy density function, α and β are material parameters for the wall, and IB is
153 the first invariant of the left Cauchy-Green deformation tensor (B). This relationship has since
154 become the *de facto* method for representing the material behaviour of aneurysm tissue [7-13]
155 in the absence of patient-specific mechanical properties. The coefficients of the strain energy
156 density function (α and β), selected for the present study, were based on the population mean
157 values ($\alpha = 0.171 N/mm^2$, and $\beta = 1.881 N/mm^2$) proposed previously [28].

158

159 *2.4 Finite element analysis model definitions*

160 To remove any variability due to loading, and to allow for comparison across patient cases, a
161 peak systolic blood pressure of 120 mm Hg (0.016 N/mm^2) was applied as an outward facing
162 uniformly distributed pressure load acting on the luminal surface of the aneurysm, as in many
163 previous studies [9, 16, 22]. The effect of wall shear stress due to blood flow was not
164 considered due to its negligible magnitude [40].

165 Residual stresses in the aortic wall, and the interaction of the aorta with the surrounding
166 structures of the body (e.g. organs and spine), were also not considered, however,
167 displacements at the distal and proximal most regions of each aneurysm were restrained, in all

168 degrees of freedom, to model attachment of the AAA to the rest of the aorta.

169 Each AAA volume mesh typically consisted of > 160,000 (C3D10H) elements. Based on

170 convergence studies the maximum allowable element edge length was set to 1.5mm. All

171 simulations were computed on a Dell Precision T7600 work station with 16 cores and 64GB

172 of ram, with typical simulation runtimes of < 2hrs (depending on simulation size). The

173 resulting contour plots of von Mises stress and the location of PWS were output for all

174 analyses.

175

176 *2.5 Geometrical analysis*

177 Triangular surface meshes representing the inner and outer aortic walls were extracted from

178 the volumetric mesh, together with values of wall stress defined at each node. The Vascular

179 Modelling Toolkit (VMTK) [41, 42] was then used to compute additional variables:

180 1. Aneurysm size, defined as the maximum diameter orthogonal to the centreline.

181 2. Wall thickness, defined as the local distance between the inner and outer wall.

182 3. Curvature, defined as the local Gaussian curvature of the outer wall.

183 4. Wall strength, estimated with the empirically determined relationship in [43]

184 5. Rupture potential index (RPI), defined as the local wall stress divided by the local wall

185 strength.

186

187 *2.6 Rupture risk calculation*

188 Failure occurs when the stress in a system exceeds its strength, at any given point. To

189 calculate the risk of failure requires knowledge of the stresses in the system and the precise

190 strength of the material it is constructed from. In this study, wall strength for each individual

191 AAA was estimated using an empirically determined relationship [43], risk of rupture was

192 then assessed using the Rupture Potential Index (RPI) [17] which is defined as the local wall
193 stress divided by the local wall strength. The returned index then indicates the potential
194 likelihood of rupture occurring, where values close to 0 indicate a relatively low risk and
195 values approaching 1 indicate a very high risk of rupture.
196

197 ## 3. RESULTS

198 Maximum diameter as measured orthogonal to the centreline of each reconstructed AAA was
199 recorded and compared to the clinically accepted ultrasound (US) derived maximum
200 diameter (Table 2). The mean difference in measurements between these two modalities was
201 6.4mm. In all but one case (patient 5) maximum diameter predictions based on CT
202 reconstructions were considerably higher than US predictions.
203 The mean wall thickness, in the region of interest (the aneurysm sac), across all PS_wall
204 models was 1.77mm ± 0.42mm. For visualisation purposes, the local variations in wall
205 thickness over the entire aneurysm for each AAA considered (for both Uni_wall and PS_wall
206 models) can be seen in Fig. 3, where blue regions indicate a thickness in the range of 0 -
207 2mm, grey regions indicate a value close to 2mm, and red regions indicate a value in the
208 range of 2 - 4mm. From the Figure it can be seen that, there is no variation in the Uni_wall
209 thickness models (1.9mm) indicated by the constant grey colour over the entire surface. In
210 comparison, each of the PS_wall cases exhibited a large amount of variation in thickness (e.g.
211 Patient 7) with alternating regions of thick and thin wall (as indicated by blue and red
212 contours respectively). Table 3 presents more quantitative information on the range of wall
213 thickness values recorded at the aneurysm sac for each AAA.
214 The peak wall stress (PWS) for Uni_wall models was 0.4905N/mm^2 (0.3495 – 0.5676
215 N/mm^2), for PS_wall models mean PWS was 0.6761N/mm^2 (0.2502 – 1.1305N/mm^2). From

216 the contour plots of stress (Fig. 4), it can be seen that in 4 out of 8 cases the assumption of a
217 uniform wall leads to an underestimation of PWS, as a result of an artificially thickened aortic
218 wall in key regions. On the other hand, in the 4 remaining cases this same assumption led to
219 an overestimation of PWS, due to the patient-specific wall being much thicker than the
220 assumed 1.9mm uniform wall. In all cases, the distribution of stress was found to be highly
221 influenced by local variations in wall thickness. Table 3 summarises the peak wall stress
222 found for each model and the percentage change in stress due to wall thickness. The
223 accompanying pie charts (Fig. 5) show the approximate region of the aneurysm in which the
224 PWS was observed, where the symbols correspond to a particular patient number as indicated
225 in Table 3. The majority of PWS was observed to occur posteriorly for the Uni_wall cases
226 [4]. Interestingly, for the PS_wall cases, the majority occurred in the anterior region, as
227 indicated by the change in location of PWS for 4 out of 8 patients between wall types (Fig. 5a
228 and Fig. 5b).
229 To further characterise the impact of wall geometry on stress distribution, the volume of the
230 aneurysm which experienced stress $\geq 0.5 N/mm^2$ was recorded for both wall types (Fig. 6a),
231 this value was then characterised as a percentage of the total volume of the aneurysm (Fig.
232 6b). From the Figures, it is clear that there is a significant increase in the overall volume of
233 the aneurysm subject to elevated stress in patients 1 – 4 when patient-specific thickness is
234 incorporated into these models. In cases where the value of PWS was quite similar (e.g.
235 patients 5 – 8), little difference was observed in the volume of the aneurysm subjected to
236 elevated stress regardless of wall type used.
237 The outer surface curvature (Gaussian curvature) of each aneurysm, for both wall types, was
238 also investigated in this study and is presented in Fig. 7. Positive curvature is indicated by red
239 regions and negative curvature is indicated by blue regions. In all cases, outer surface

curvature was found to be quite similar for both wall types, with the AAA sac being characterised by high positive curvature, and the transition zones (shoulder region and above iliac bifurcation) being characterised by high negative curvature. Only minor differences were observed in surface curvature, due to local surface features present in the PS_wall cases.

The rupture risk of each AAA was assessed in this study using the rupture potential index (RPI). Three-dimensional contour plots of RPI are presented for each AAA in Fig. 8. It can be seen by comparing Fig. 8 and Fig. 4 that areas of increased rupture risk co-locate with regions of high stress. It can also be seen that both Uni_wall and PS_wall variations having very different distributions of RPI. By examining the maximum RPI for each AAA it can be seen that wall type has a significant impact on the perceived risk of aneurysm rupture (Fig. 9), particularly in patients 1, 2, and 4 where rupture risk more than doubled after incorporation of PS wall thickness. In Patients 3, 6 and 8, patient-specific geometry only led to a marginal increase in rupture risk, while in Patients 5 and 7 a slight reduction in maximum rupture risk was observed.

4. DISCUSSION

This study aimed to assess the importance of wall thickness in a small population ($n = 8$) of abdominal aortic aneurysms (AAAs) which physically lacked intraluminal thrombus. This was achieved by comparing patient-specific and uniform wall thickness models of each individual aneurysm investigated. The influence of wall thickness on clinically relevant markers such as AAA curvature, peak wall stress (PWS) and rupture risk index (RPI) was then assessed.

A small number of previous studies have attempted to discern the role of wall thickness in PWS and rupture risk predictions [7, 9-11, 13, 21, 28, 33-38]. In their rupture risk equation,

Li and Kleinstreuer [34] introduced an approximation of PS wall thickness using a curve-fitted correlation, however, their simplified approach is unable to deal with areas of extreme curvature/angulation. Studies by Raghavan et al. [28], Wang et al. [10], and Venkatasubramaniam et al. [13] detailed models which varied in thickness in the radial direction (only) based on patient-specific measurements from CT, yet each model still maintained a uniform cross-section. Work by Scotti et al. [21, 37] improved on this by varying thickness in both the radial and axial directions, however, at any given cross-section the thickness remained constant around the circumference. A more recent study by Gasser et al. [33], implemented a smart algorithm which varied the AAA wall thickness between 1.5 mm (at thrombus-free) and 1.13 mm (at covered sites), in effect approximating a physiological type wall thickness based on the amount of thrombus adjacent to the wall at a given location. Nevertheless, in the absence of thrombus, this method would again result in a uniform wall thickness being applied. As a result, these methods do not fully characterise the significant local variations in thickness which may be encountered due to the heterogeneity of the aneurysm wall [29, 30]. It wasn't until the work of Shum et al. [38] that a physiologically representative method was developed for estimating patient-specific wall thickness based on manually trained neural networks and features extracted from the CT images, thus meaning a thickness could vary in the axial, radial and circumferential directions. Their method has formed the basis of several later studies e.g. [11, 36]. Similarly Shang et al. [7] employed a series of custom algorithms to extrapolate a "patient-specific" variable wall geometry from CT data, based on the grayscale intensity values of individual pixels. However, such methods remain open to ambiguity as to what constitutes wall and thrombus in such a highly heterogeneous structure. Any misidentification of these structures at input could significantly alter the estimated wall thickness and as a result the projected clinical outcomes. In this study

288 no such algorithms were applied, instead wall thickness was obtained directly from CT
289 through careful selection of patient type. As wall thickness was free to vary in line with the
290 CT images this allowed for non-uniformity to occur in all directions, and fine local features
291 (e.g. very thick and extremely thin) to be resolved, as can be seen in Fig. 3. An aspect not
292 typically accounted for by "black box" wall estimation algorithms; as such features may be
293 obscured by the presence of intraluminal thrombus on the CT images or because they don't fit
294 within the minimum specified parameters for wall thickness often employed in such
295 estimation algorithms.
296 The current gold standard for AAA assessment is the 55mm maximum diameter criterion. In
297 this study, maximum diameter values were extracted from the CT based models and
298 compared to the clinically obtained US measurements, as was shown in Table 2, these values
299 varied considerably (-1mm to 12mm). Only some of this error in measurement could be
300 attributed to differences in measurement plane taken, e.g. anterior-posterior measurement vs.
301 maximal measurement in any other direction [35].
302 Based on the maximum diameter criterion (55mm) only Patients 3 and 7, from the current
303 study, would be prioritised for surgery according to the ultrasound measurements, whereas the
304 CT based diameter measurements identify an additional case over the 55mm threshold
305 (Patient 1). Furthermore, CT measurements highlight two more cases very close to the
306 threshold for intervention (Patients 4 and 8). These points underscore the unsuitability of the
307 current diameter based intervention criterion and support the need for an improved marker for
308 AAA rupture risk.
309 Peak wall stress (PWS) has been shown to be an improved marker of rupture risk, when
310 compared with the traditional maximum diameter measurement [24]. In this study, the inter-
311 patient variability in terms of both location (Fig. 5a) and magnitude of PWS (σ_{mean} = 0.4905 ±

312 0.0850N/mm^2) was found to be very low in uniform wall thickness (Uni_wall) models, with
313 PWS predominately located in the posterior region, additionally the range of PWS observed
314 in the Uni_wall models was consistent with many previous studies [8, 44]. In contrast,
315 significantly higher values of PWS (by as much as 55%) were observed in half of the patients
316 investigated after incorporation of patient-specific (PS) wall thickness. A similar observation
317 was reported by Shang et al. [7] though to a lesser degree (10 – 12% increase in PWS),
318 possibly due to the presence of thrombus in the patients recruited in their study. In the present
319 study, all patients lack this protective buffer and as a consequence are subject to much higher
320 stresses [18, 25]. Furthermore, the inter-patient variability in the location (Fig. 5b) and
321 magnitude of PWS (σ_{mean} = 0.6761 ± 0.3410N/mm^2) in PS_wall models was found to be quite
322 high in comparison to the Uni_wall models. These findings highlight how the uniform wall
323 assumption may obscure important clinically relevant information through artificial
324 thickening of the aneurysm wall, thus removing locally thinned regions and biasing PWS
325 locations and magnitudes. In addition, contrary to previously reported findings [9, 37, 45],
326 wall thickness was also observed to influence the distribution of stress within the wall of the
327 aneurysm. In particular, dramatic changes in wall stress distribution were observed, between
328 the two wall types, where excessive thinning or thickening of the aortic wall occurred locally.
329 It has been shown previously, that a reduction or change in wall thickness can lead to an
330 increase in PWS [11, 13, 21, 28, 37], what has not been discussed is the impact that these
331 changes may have on the volume over which this elevated stress acts. In the present study, the
332 volume of stress ≥ 0.5N/mm^2 in each AAA was investigated (Fig. 6a) and expressed as a
333 percentage of the total AAA volume (Fig. 6b). These results highlight a dramatic difference
334 in terms of the proportion of the aneurysm under elevated stress, with patients 1 – 4
335 experiencing significant increases in volume when PS wall thickness is considered over

336 uniform wall thickness. This fact is of importance as rupture occurs when the wall stress
337 exceeds the wall strength, which may not necessarily be at the location of PWS, while the
338 wall stress may be high in a locally thinned region this may be counterbalanced by a high wall
339 strength [16], on the other hand a relatively thick section of wall may have a much lower wall
340 strength [18, 31, 45] and therefore fail at a much lower value of wall stress. Consequently,
341 aneurysms with elevated stress acting over a larger volume may have an increased risk of
342 rupturing at these secondary locations (e.g. locations not associated with peak stress).
343 Previous studies have suggested a link between curvature and wall stress [46]. In this study,
344 the wall type (Uni_wall or PS_wall) was found to have minimal impact on curvature itself,
345 with little variation observed between wall types. However, wall thickness was observed to
346 have a dominant influence on correlations of curvature with wall stress. By comparing
347 curvature (Fig. 7) with the contour plots of stress presented in Fig. 4 it can be seen that
348 negative curvature co-located with regions of increased stress (i.e. at inflection points), in the
349 Uni_wall cases. However, when patient-specific wall thickness was considered the correlation
350 between curvature and stress was less clear, with high stress found to co-locate with a mixture
351 of negative and positive curvature (e.g. Patients 3, 4 and 7).
352 The rupture potential index (RPI), established by Vande Geest et al. [17] returns an estimate
353 of rupture risk based on the wall stress predicted by FE and the wall strength obtained using a
354 mathematical model which incorporates geometric and patient information to approximate the
355 distribution of strength in the wall for a given aneurysm. Values close to 0 indicate a
356 relatively low risk of rupture, whereas values close to 1 indicate an increased risk of rupture.
357 In the present study, RPI was used as a means to investigate the implications of PS wall
358 thickness on rupture risk in a more quantifiable manner. Wall thickness was observed to have
359 a profound impact on the predicted rupture risk for certain patients (Patients 1 – 4), as shown

360 in Fig. 9. Moving from a Uni_wall to a PS_wall in some instances (Patients 1, 2, and 4) more
361 than doubled the likelihood of rupture occurring. It is important to note that, under the
362 uniform wall assumption these cases would have been dismissed as borderline, while in
363 reality they are high risk, as indicated by a RPI values in excess of 0.5. Interestingly these
364 particular cases (Patients 1, 2, and 4) all have maximum diameters below the 55mm criterion
365 used clinically to discern at risk aneurysms. Conversely, some of the lowest reported RPI
366 values occurred in patients with large AAAs (patients 7 and 8). Of the previous studies which
367 incorporated some form of variable wall thickness [7, 13, 21, 28, 36, 37] only one such study
368 investigated rupture risk [36]. In their study Martufi and colleagues examined the RPI of a
369 single patient-specific AAA with a variable wall thickness, and found that rupture risk was
370 distributed in a complex manner across the aneurysm (similar to the findings of this
371 study).However, the influence of wall thickness on predicted RPI was not assessed in their
372 study as no direct comparison of RPI with a uniform wall thickness model was presented.
373 The present study has focussed on patients with aneurysms which physically lacked thrombus
374 formations. Nevertheless, it is recognised that the majority of aneurysm encountered clinically
375 do have some degree of thrombus [7], the influence of wall thickness under such
376 circumstances is still significant, however, in comparison to the findings of the present study
377 its influence is much reduced. It is therefore suggested that, PS wall thickness may be more
378 influential in patients who lack thrombus.
379 In this study, all AAAs were modelled as isotropic, non-linear, hyperelastic, and
380 incompressible. In reality, the aorta is highly anisotropic; however, the assumption of isotropy
381 is considered valid in AAAs, where the wall tissue is fibrous [47]. Similarly, a lack of
382 information regarding patient-specific wall strength necessitated the use of a mathematical
383 model for strength estimation [43], which takes into account clinically relevant variables such

384 as thrombus thickness, aorta dilation, family history, and sex. However, as the 8 patients in
385 this study are thrombus free, the estimated strength varies predominately with local AAA wall
386 dilation, and global factors such as sex and family history. This leads to a very uniform
387 distribution of strength around the circumference of the sac (see supplementary text).
388 Realistically, strength properties may vary considerably in different regions (e.g.
389 anterior/posterior) of the aneurysm [31, 47, 48]. Additionally, cyclical fatigue failure may also
390 cause AAA structures to fail at much lower values of stress [49] in vivo, than presented in
391 these static analyses.
392 In this study, loading consisted of a uniformly distributed static pressure applied to the
393 luminal surface of each AAA. In the aorta, the pressure on the wall is dynamic and changes
394 throughout the cardiac cycle, and as a result of flow instabilities. This could lead to a non-
395 uniform distribution of pressure and as a consequence, a very different distribution of stress
396 than observed in the current study. However, previous studies have shown that while overall
397 distribution of stress changes, the actual influence on PWS is less than 4% [37, 40, 50].
398 Other factors such as inclusion of: pre-stressing [25], calcification [51-53], spinal contact and
399 soft tissue constraints [54, 55], also play a role in altering the mechanical environment in the
400 AAA and may need to be considered depending on the application of the model.
401 While these limitations are important from the perspective of precision in rupture risk
402 prediction for a given patient, they are unlikely to influence the overall outcomes relating to
403 wall thickness presented in this work due to the comparative nature of the study.
404
405 *4.1 Conclusions*
406 This study has highlighted the impact of one possible source of variation, patient-specific vs.
407 uniform aneurysm wall thickness, which has the potential to seriously affect predicted clinical

outcomes.

The findings of this study have shown that incorporation of PS wall thickness dramatically influences; the overall distribution of stress, its correlation with curvature, the location and magnitude of peak wall stress (PWS), the volume of the AAA wall under elevated stress, and the calculated rupture risk index for each AAA. Uniform wall thickness, has been found to be inadequate when investigating outcomes in patients with no intraluminal thrombus , as the uniform wall removed key local geometrical features (e.g. very thick and very thin regions of wall), which have a significant influence on risk estimation. This highlights the sensitivity of standard rupture risk markers to the specific wall thickness strategy employed.

Furthermore, this study represents a key first step in establishing a set of ground truth models with which to verify and validate the output of wall thickness estimation algorithms, and in the future, wall thickness measurements obtained from multimodal image reconstructions, paving the way for studies which incorporate such techniques to assess true patient-specific wall thickness in a wider selection of patients with intraluminal thrombus formations.

5. ACKNOWLEDGEMENTS

The authors would like to acknowledge Scott I. Semple, Tom J. MacGillivray, and Julian Sparrow of the Clinical Research Imaging Centre, Edinburgh for maintaining and facilitating access to the medical imaging data from the MA3RS clinical trial.

434 6. REFERENCES

435 [1] Mitchell D, Hindley H, Naylor R, Wyatt M, Loftus I. The Abdominal Aortic Aneurysm
436 Quality Improvement Programme The Vascular Society of Great Britian & Ireland; 2012.
437 [2] Mortality results for randomised controlled trial of early elective surgery or
438 ultrasonographic surveillance for small abdominal aortic aneurysms. The Lancet.
439 1998;352:1649-55.
440 [3] Brown LC, Powell JT. Risk factors for aneurysm rupture in patients kept under ultrasound
441 surveillance. UK Small Aneurysm Trial Participants. Annals of surgery. 1999;230:289-96;
442 discussion 96-7.
443 [4] Darling RC, Messina CR, Brewster DC, Ottinger LW. Autopsy study of unoperated
444 abdominal aortic aneurysms. The case for early resection. Circulation. 1977;56:II161-4.
445 [5] Nicholls SC, Gardner JB, Meissner MH, Johansen KH. Rupture in small abdominal aortic
446 aneurysms. Journal of vascular surgery. 1998;28:884-8.
447 [6] Lederle FA, Wilson SE, Johnson GR, Reinke DB, Littooy FN, Acher CW, et al.
448 Immediate Repair Compared with Surveillance of Small Abdominal Aortic Aneurysms. New
449 England Journal of Medicine. 2002;346:1437-44.
450 [7] Shang EK, Nathan DP, Woo EY, Fairman RM, Wang GJ, Gorman RC, et al. Local wall
451 thickness in finite element models improves prediction of abdominal aortic aneurysm growth.
452 Journal of vascular surgery. 2013.
453 [8] Doyle B, Callanan A, McGloughlin T. A comparison of modelling techniques for
454 computing wall stress in abdominal aortic aneurysms. BioMedical Engineering OnLine.
455 2007;6:38.
456 [9] Xiong J, Guo W, Wang J, Zhou W. Effects of Wall Thickness on Stress Distribution in
457 Patient-Specific Models of Abdominal Aortic Aneurysm. Biomedical Engineering and

458 Informatics, 2009 BMEI '09 2nd International Conference on2009. p. 1-3.
459 [10] Wang DHJ, Makaroun MS, Webster MW, Vorp DA. Effect of intraluminal thrombus on
460 wall stress in patient-specific models of abdominal aortic aneurysm. Journal of vascular
461 surgery. 2002;36:598-604.
462 [11] Raut SS, Jana A, De Oliveira V, Muluk SC, Finol EA. The Importance of Patient-
463 Specific Regionally Varying Wall Thickness in Abdominal Aortic Aneurysm Biomechanics.
464 Journal of Biomechanical Engineering. 2013;135:081010-.
465 [12] Fillinger MF, Raghavan ML, Marra SP, Cronenwett JL, Kennedy FE. In vivo analysis of
466 mechanical wall stress and abdominal aortic aneurysm rupture risk. Journal of vascular
467 surgery. 2002;36:589-97.
468 [13] Venkatasubramaniam AK, Fagan MJ, Mehta T, Mylankal KJ, Ray B, Kuhan G, et al. A
469 Comparative Study of Aortic Wall Stress Using Finite Element Analysis for Ruptured and
470 Non-ruptured Abdominal Aortic Aneurysms. European Journal of Vascular and Endovascular
471 Surgery. 2004;28:168-76.
472 [14] Hirose Y, Takamiya M. Growth curve of ruptured aortic aneurysm. The Journal of
473 cardiovascular surgery. 1998;39:9-13.
474 [15] Richards JM, Semple SI, MacGillivray TJ, Gray C, Langrish JP, Williams M, et al.
475 Abdominal aortic aneurysm growth predicted by uptake of ultrasmall superparamagnetic
476 particles of iron oxide: a pilot study. Circulation Cardiovascular imaging. 2011;4:274-81.
477 [16] Doyle BJ, Callanan A, Walsh M, Grace P, McGloughlin T. A finite element analysis
478 rupture index (FEARI) as an additional tool for abdominal aortic aneurysm rupture prediction.
479 Vascular Disease Prevention. 2009;6:114 - 21.
480 [17] Vande Geest JP, Di Martino ES, Bohra A, Makaroun MS, Vorp DA. A Biomechanics-
481 Based Rupture Potential Index for Abdominal Aortic Aneurysm Risk Assessment. Annals of

482 the New York Academy of Sciences. 2006;1085:11-21.
483 [18] Vorp DA, Geest JPV. Biomechanical Determinants of Abdominal Aortic Aneurysm
484 Rupture. Arteriosclerosis, Thrombosis, and Vascular Biology. 2005;25:1558-66.
485 [19] Polzer S, Gasser TC, Swedenborg J, Bursa J. The Impact of Intraluminal Thrombus
486 Failure on the Mechanical Stress in the Wall of Abdominal Aortic Aneurysms. European
487 Journal of Vascular and Endovascular Surgery. 2011;41:467-73.
488 [20] Doyle BJ, Callanan A, Burke PE, Grace PA, Walsh MT, Vorp DA, et al. Vessel
489 asymmetry as an additional diagnostic tool in the assessment of abdominal aortic aneurysms.
490 Journal of vascular surgery. 2009;49:443-54.
491 [21] Scotti C, Shkolnik A, Muluk S, Finol E. Fluid-structure interaction in abdominal aortic
492 aneurysms: effects of asymmetry and wall thickness. BioMedical Engineering OnLine.
493 2005;4:64.
494 [22] Vorp DA, Raghavan ML, Webster MW. Mechanical wall stress in abdominal aortic
495 aneurysm: Influence of diameter and asymmetry. Journal of vascular surgery. 1998;27:632-9.
496 [23] Volokh KY, Vorp DA. A model of growth and rupture of abdominal aortic aneurysm. J
497 Biomech. 2008;41:1015-21.
498 [24] Malkawi AH, Hinchliffe RJ, Xu Y, Holt PJ, Loftus IM, Thompson MM. Patient-specific
499 biomechanical profiling in abdominal aortic aneurysm development and rupture. Journal of
500 vascular surgery. 2010;52:480-8.
501 [25] Reeps C, Gee M, Maier A, Gurdan M, Eckstein H-H, Wall WA. The impact of model
502 assumptions on results of computational mechanics in abdominal aortic aneurysm. Journal of
503 vascular surgery. 2010;51:679-88.
504 [26] Taylor CA, Figueroa CA. Patient-Specific Modeling of Cardiovascular Mechanics.
505 Annual Review of Biomedical Engineering. 2009;11:109-34.

506 [27] Wang G, Zhang J, Gao H, Weir V, Yu H, Cong W, et al. Towards Omni-Tomography—
507 Grand Fusion of Multiple Modalities for Simultaneous Interior Tomography. PLoS ONE.
508 2012;7:e39700.
509 [28] Raghavan ML, Vorp DA, Federle MP, Makaroun MS, Webster MW. Wall stress
510 distribution on three-dimensionally reconstructed models of human abdominal aortic
511 aneurysm. Journal of vascular surgery. 2000;31:760-9.
512 [29] Sumner DS, Hokanson DE, Strandness DEJ. Stress Strain Characteristics and Collagen
513 Elastin Content of Abdominal Aortic Aneurysms. Surgery Gynecology and Obstetrics.
514 1970;130:459-66.
515 [30] Kazi M, Thyberg J, Religa P, Roy J, Eriksson P, Hedin U, et al. Influence of intraluminal
516 thrombus on structural and cellular composition of abdominal aortic aneurysm wall. Journal
517 of vascular surgery. 2003;38:1283-92.
518 [31] Raghavan ML, Kratzberg J, Castro de Tolosa EM, Hanaoka MM, Walker P, da Silva ES.
519 Regional distribution of wall thickness and failure properties of human abdominal aortic
520 aneurysm. Journal of Biomechanics. 2006;39:3010-6.
521 [32] Humphrey JD, Holzapfel GA. Mechanics, mechanobiology, and modeling of human
522 abdominal aorta and aneurysms. Journal of Biomechanics. 2012;45:805-14.
523 [33] Gasser TC, Auer M, Labruto F, Swedenborg J, Roy J. Biomechanical Rupture Risk
524 Assessment of Abdominal Aortic Aneurysms: Model Complexity versus Predictability of
525 Finite Element Simulations. European Journal of Vascular and Endovascular Surgery.
526 2010;40:176-85.
527 [34] Li Z, Kleinstreuer C. A new wall stress equation for aneurysm-rupture prediction. Ann
528 Biomed Eng. 2005;33:209-13.
529 [35] Manning BJ, Kristmundsson T, Sonesson B, Resch T. Abdominal aortic aneurysm

530 diameter: A comparison of ultrasound measurements with those from standard and three-
531 dimensional computed tomography reconstruction. Journal of vascular surgery. 2009;50:263-
532 8.
533 [36] Martufi G, Satriano A, Moore RD, Vorp DA, Di Martino ES. Local Quantification of
534 Wall Thickness and Intraluminal Thrombus Offer Insight into the Mechanical Properties of
535 the Aneurysmal Aorta. Ann Biomed Eng. 2015;43:1759-71.
536 [37] Scotti CM, Jimenez J, Muluk SC, Finol EA. Wall stress and flow dynamics in abdominal
537 aortic aneurysms: finite element analysis vs. fluid–structure interaction. Computer Methods in
538 Biomechanics and Biomedical Engineering. 2008;11:301-22.
539 [38] Shum J, DiMartino ES, Goldhamme A, Goldman DH, Acker LC, Patel G, et al.
540 Semiautomatic vessel wall detection and quantification of wall thickness in computed
541 tomography images of human abdominal aortic aneurysms. Medical Physics. 2010;37:638-48.
542 [39] McBride OMB, Berry C, Burns P, Chalmers RTA, Doyle B, Forsythe R, et al. MRI using
543 ultrasmall superparamagnetic particles of iron oxide in patients under surveillance for
544 abdominal aortic aneurysms to predict rupture or surgical repair: MRI for abdominal aortic
545 aneurysms to predict rupture or surgery—the MA3RS study. Open Heart. 2015;2.
546 [40] Fraser KH, Li M-X, Lee WT, Easson WJ, Hoskins PR. Fluid—structure interaction in
547 axially symmetric models of abdominal aortic aneurysms. Proceedings of the Institution of
548 Mechanical Engineers, Part H: Journal of Engineering in Medicine. 2009;223:195-209.
549 [41] Antiga L, Piccinelli M, Botti L, Ene-Iordache B, Remuzzi A, Steinman D. An image-
550 based modeling framework for patient-specific computational hemodynamics. Med Biol Eng
551 Comput. 2008;46:1097-112.
552 [42] Piccinelli M, Veneziani A, Steinman DA, Remuzzi A, Antiga L. A Framework for
553 Geometric Analysis of Vascular Structures: Application to Cerebral Aneurysms. Medical

554 Imaging, IEEE Transactions on. 2009;28:1141-55.
555 [43] Vande Geest J, Wang DJ, Wisniewski S, Makaroun M, Vorp D. Towards A Noninvasive
556 Method for Determination of Patient-Specific Wall Strength Distribution in Abdominal Aortic
557 Aneurysms. Ann Biomed Eng. 2006;34:1098-106.
558 [44] Fillinger MF, Marra SP, Raghavan ML, Kennedy FE. Prediction of rupture risk in
559 abdominal aortic aneurysm during observation: Wall stress versus diameter. Journal of
560 vascular surgery. 2003;37:724-32.
561 [45] Thubrikar MJ, Al-Soudi J, Robicsek F. Wall stress studies of abdominal aortic aneurysm
562 in a clinical model. Ann Vasc Surg. 2001;15:355-66.
563 [46] Leung J, Nyilas RD, Ng SML, Xu XY. Towards a new geometric approach to assess the
564 risk of rupture of abdominal aortic aneurysms using patient specific modeling. The 2005
565 Summer Bioengineering Conference. Abstract SBC2005-I212005.
566 [47] Raghavan ML, Webster M, Vorp D. Ex vivo biomechanical behavior of abdominal aortic
567 aneurysm: Assessment using a new mathematical model. Ann Biomed Eng. 1996;24:573-82.
568 [48] Thubrikar MJ, Labrosse M, Robicsek F, Al-Soudi J, Fowler B. Mechanical properties of
569 abdominal aortic aneurysm wall. Journal of medical engineering & technology. 2001;25:133-
570 42.
571 [49] Gasser TC, Görgülü G, Folkesson M, Swedenborg J. Failure properties of intraluminal
572 thrombus in abdominal aortic aneurysm under static and pulsating mechanical loads. Journal
573 of vascular surgery. 2008;48:179-88.
574 [50] Leung J, Wright A, Cheshire N, Crane J, Thom S, Hughes A, et al. Fluid structure
575 interaction of patient specific abdominal aortic aneurysms: a comparison with solid stress
576 models. BioMedical Engineering OnLine. 2006;5:33.
577 [51] Li ZY, J UK-I, Tang TY, Soh E, See TC, Gillard JH. Impact of calcification and

578 intraluminal thrombus on the computed wall stresses of abdominal aortic aneurysm. Journal
579 of vascular surgery. 2008;47:928-35.
580 [52] Speelman L, Bohra A, Bosboom EMH, Schurink GWH, van de Vosse FN, Makaroun
581 MS, et al. Effects of Wall Calcifications in Patient-Specific Wall Stress Analyses of
582 Abdominal Aortic Aneurysms. Journal of Biomechanical Engineering. 2006;129:105-9.
583 [53] O'Leary SA, Mulvihill JJ, Barrett HE, Kavanagh EG, Walsh MT, McGloughlin TM, et
584 al. Determining the influence of calcification on the failure properties of abdominal aortic
585 aneurysm (AAA) tissue. Journal of the Mechanical Behavior of Biomedical Materials.
586 2015;42:154-67.
587 [54] Gasbarro MD, Shimada K, Di Martino ES. mechanics of abdominal aortic aneurysm.
588 European Journal of Computational Mechanics/Revue Européenne de Mécanique Numérique.
589 2007;16:337-63.
590 [55] Zeinali-Davarani S, Dupay A, Baek S, Lee W. Interactions with spine during abdominal
591 aortic aneurysm enlargement and its biomechanical effects. the ASME 2012 Summer
592 Bioengineering Conference. Fajardo, Puerto Rico2012.
593
594
595
596
597
598
599
600
601

602 7. LEGEND TO FIGURES

603 Figure 1: Comparison of two AAAs one with intraluminal thrombus (a) and one without (b).
604 The blue line in the top panel indicates the location of the cross-sectional slices presented for
605 each AAA (middle panel). The bottom panel then presents a zoomed in view of each cross-
606 sectional slice.
607
608 Figure 2: Model generation workflow outlining the major steps required to convert medical
609 scan data into patient-specific finite element models of abdominal aortic aneurysms.
610
611 Figure 3: Contour plots of wall thickness distribution for both Uniform (left) and Patient-
612 specific (right) cases.
613
614 Figure 4: Contour plots showing the magnitude and distribution of wall stress (von Mises) for
615 both Uniform (left) and Patient-specific (right) wall thickness cases.
616
617 Figure 5: Charts showing the approximate location of PWS for a) the uniform wall, and b) PS
618 wall models.
619
620 Figure 6: Charts showing a) volume of the AAA which experiences stress above 0.5 N/mm^2,
621 and b) this volume expressed as a percentage of the total AAA volume.
622
623 Figure 7: Comparison of outer wall curvature for both Uniform (left) and Patient-specific
624 (right) wall thickness cases.
625
626 Figure 8: Comparison of outer wall RPI for both Uniform (left) and Patient-specific (right)
627 wall thickness cases.
628
629 Figure 9: Graph showing calculated maximum rupture risk index for both wall types using the
630 RPI method, for all patients investigated. The dashed black line represents the point after
631 which risk of rupture increases significantly.
632

633 **Table 1:** Patient details for each of the reconstructed aneurysms. Strength estimation relies
634 on knowledge of patient family history of AAAs, where this information was unavailable a
635 worst case scenario of yes was assumed as indicated by the accompanying *.

Patient	Age	Gender	Family History	Diameter from US (mm)	AAA Type
1	83	Male	No	44	Fusiform
2	80	Male	Yes	40	Fusiform
3	81	Male	No	59	Fusiform
4	82	Female	No	44	Fusiform
5	70	Male	No	41	Saccular
6	64	Male	Yes*	36	Saccular
7	65	Male	No	59	Fusiform
8	81	Male	No	47	Fusiform

636
637
638
639
640
641

642 **Table 2:** Comparison of clinically accepted maximum diameter measurements from

643 ultrasound, with maximum diameter measurements from CT reconstructions of each patient.

Patient number	Diameter (mm)		Difference (mm)
	From US	From CT	
1	44	56	12
2	40	47	7
3	59	64	5
4	44	53	9
5	41	40	-1
6	36	43	7
7	59	66	7
8	47	52	5

644

645

646

647

648

649

650

651 **Table 3:** Highlights the difference in wall thickness observed between wall types and the

652 corresponding PWS for each patient investigated.

Patient ID	Chart Symbol (Fig. 5)	Uni wall	PS wall	Wall thickness (mm)	PWS (N/mm^2)	% change in PWS
1	○	X		1.9	0.5676	-43.42
			X	1.35 – 2.01	1.0031	
2	▭	X		1.9	0.5133	-54.60
			X	1.33 – 2.45	1.1305	
3	✖	X		1.9	0.5181	-32.99
			X	0.96 – 1.64	0.7732	
4	✚	X		1.9	0.5622	-43.34
			X	0.90 – 1.39	0.9923	
5	◇	X		1.9	0.4109	4.18
			X	1.31 – 1.96	0.3944	
6	□	X		1.9	0.3495	39.69
			X	2.01 – 2.77	0.2502	
7	△	X		1.9	0.5042	14.67
			X	1.66 - 2.68	0.5039	
8	⌊	X		1.9	0.4244	17.42
			X	1.67 - 2.19	0.36144	

653

654

655

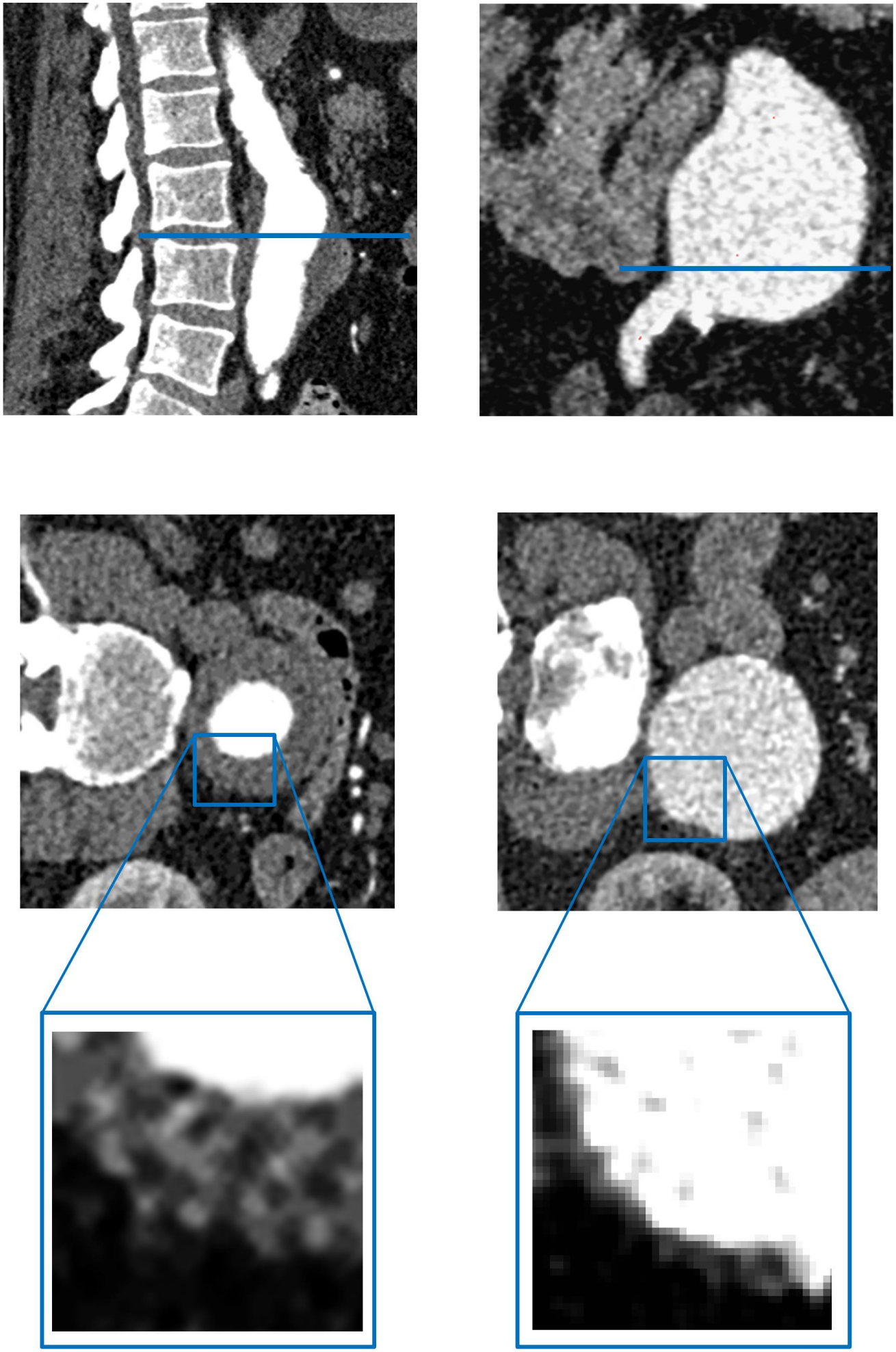

a) b)

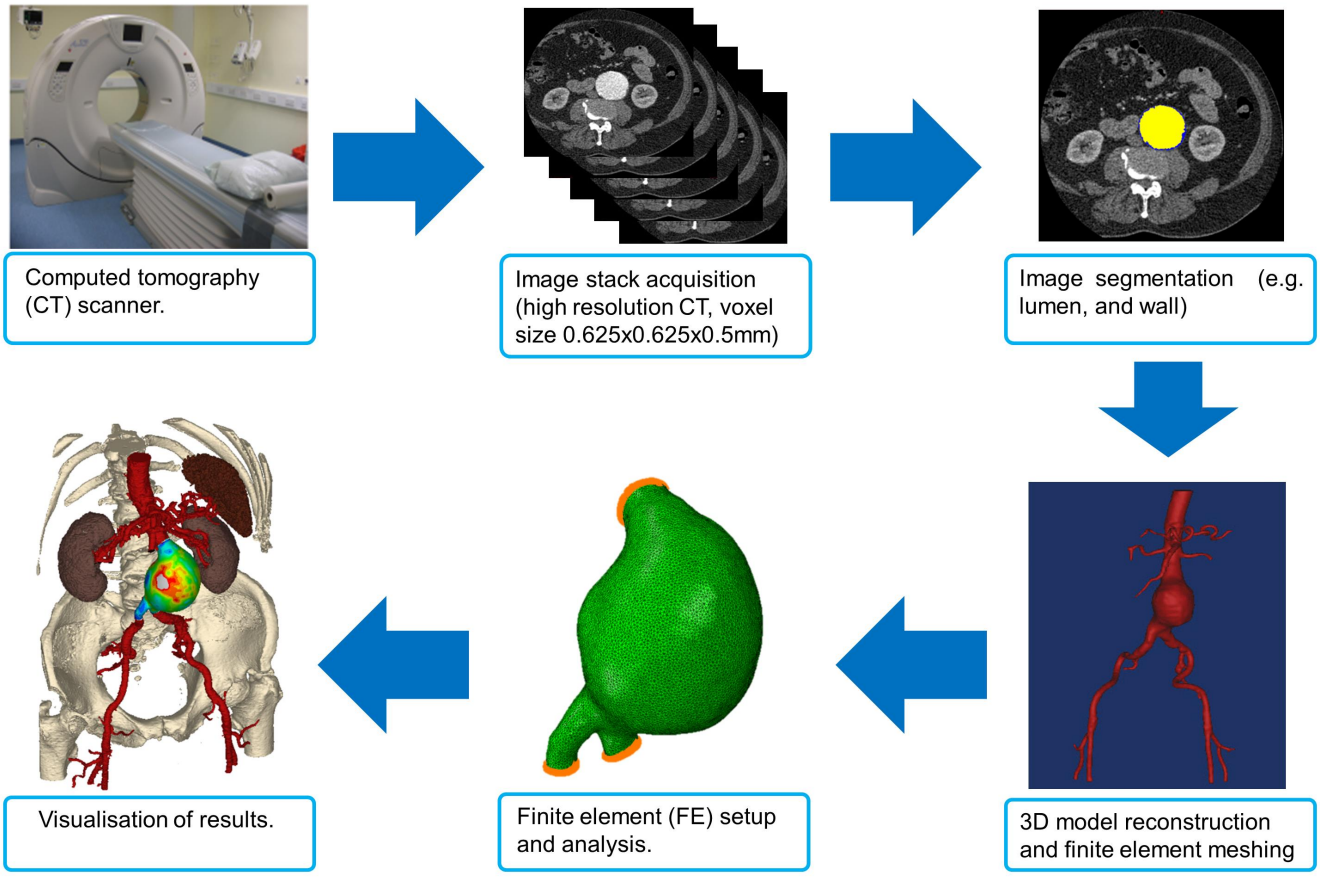
Computed tomography (CT) scanner.
Image stack acquisition (high resolution CT, voxel size 0.625x0.625x0.5mm)
Image segmentation (e.g. lumen, and wall)
3D model reconstruction and finite element meshing
Finite element (FE) setup and analysis.
Visualisation of results.

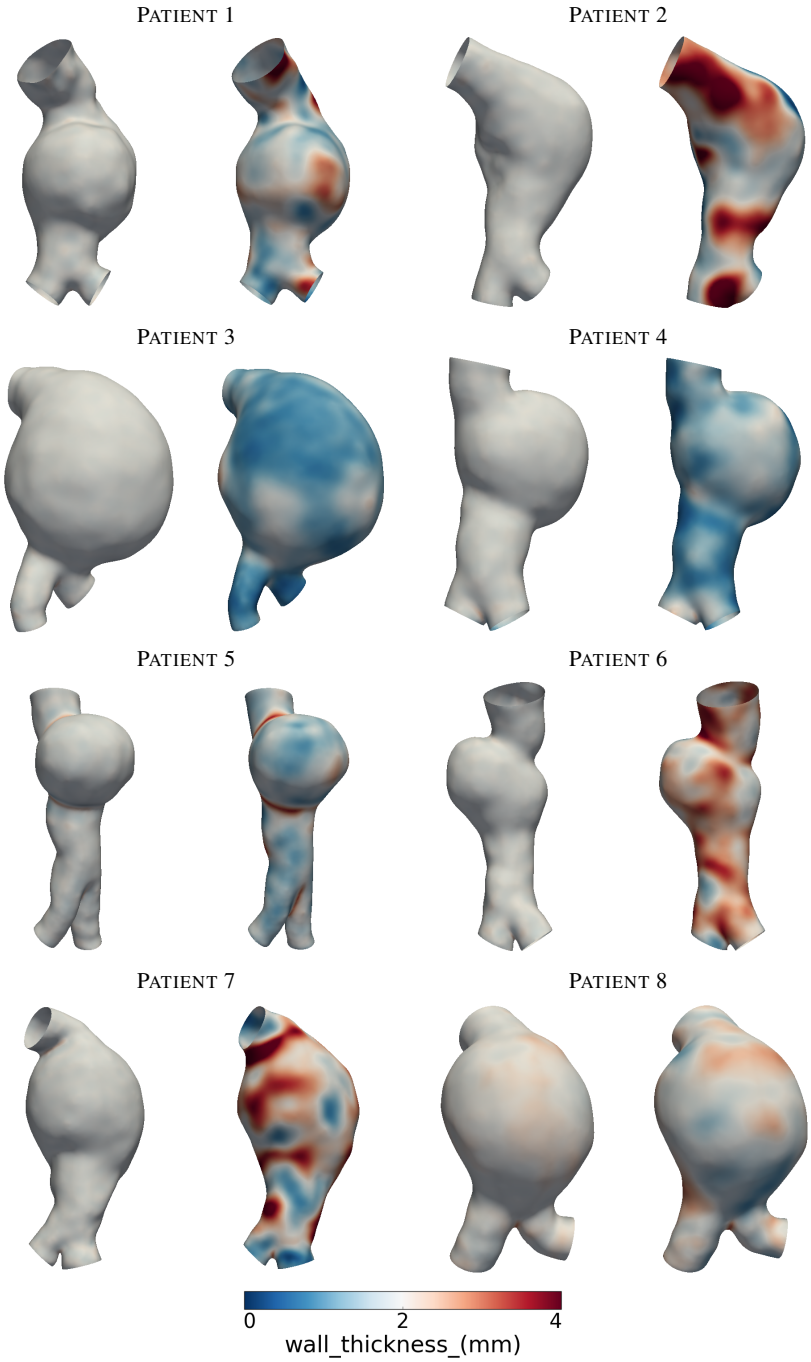
PATIENT 1
PATIENT 2
PATIENT 3
PATIENT 4
PATIENT 5
PATIENT 6
PATIENT 7
PATIENT 8
0
2
4
wall_thickness_(mm)

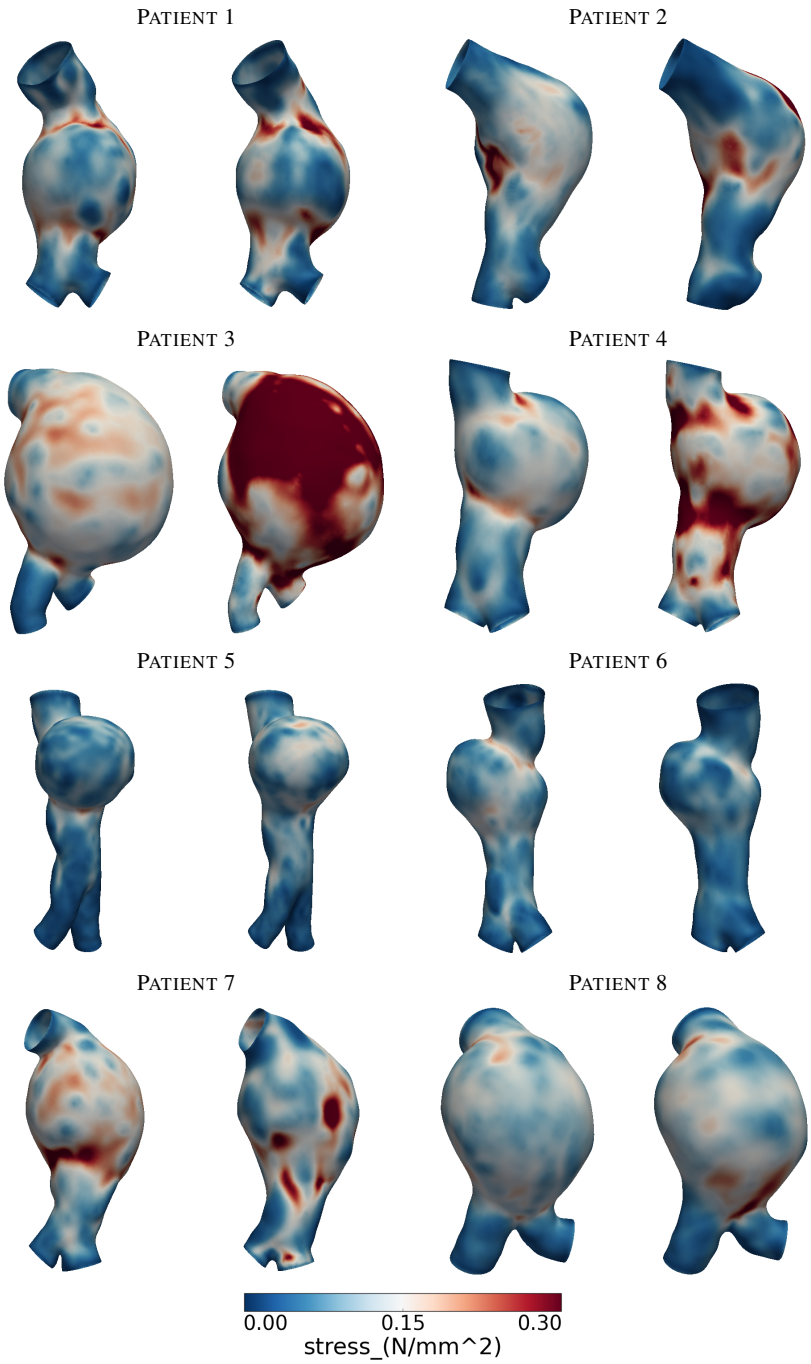
PATIENT 1
PATIENT 2
PATIENT 3
PATIENT 4
PATIENT 5
PATIENT 6
PATIENT 7
PATIENT 8
0.00
0.15
0.30
stress_(N/mm^2)

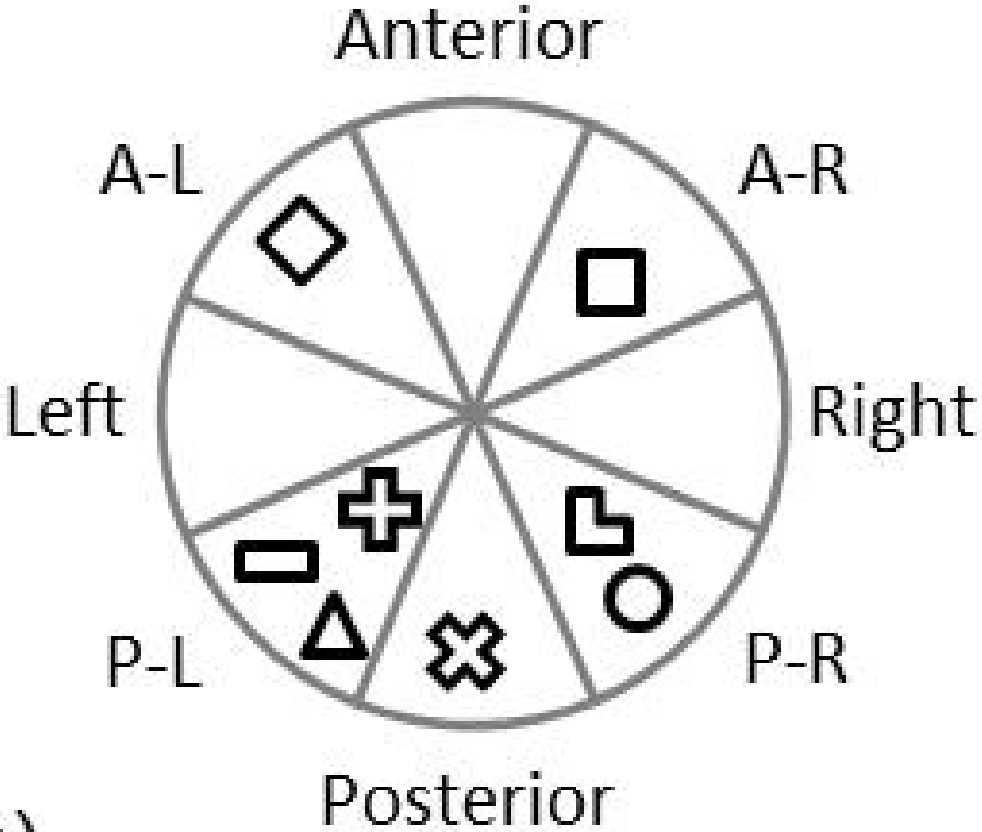
Anterior
A-L
A-R
Left
Right
P-L
P-R
Posterior

a)

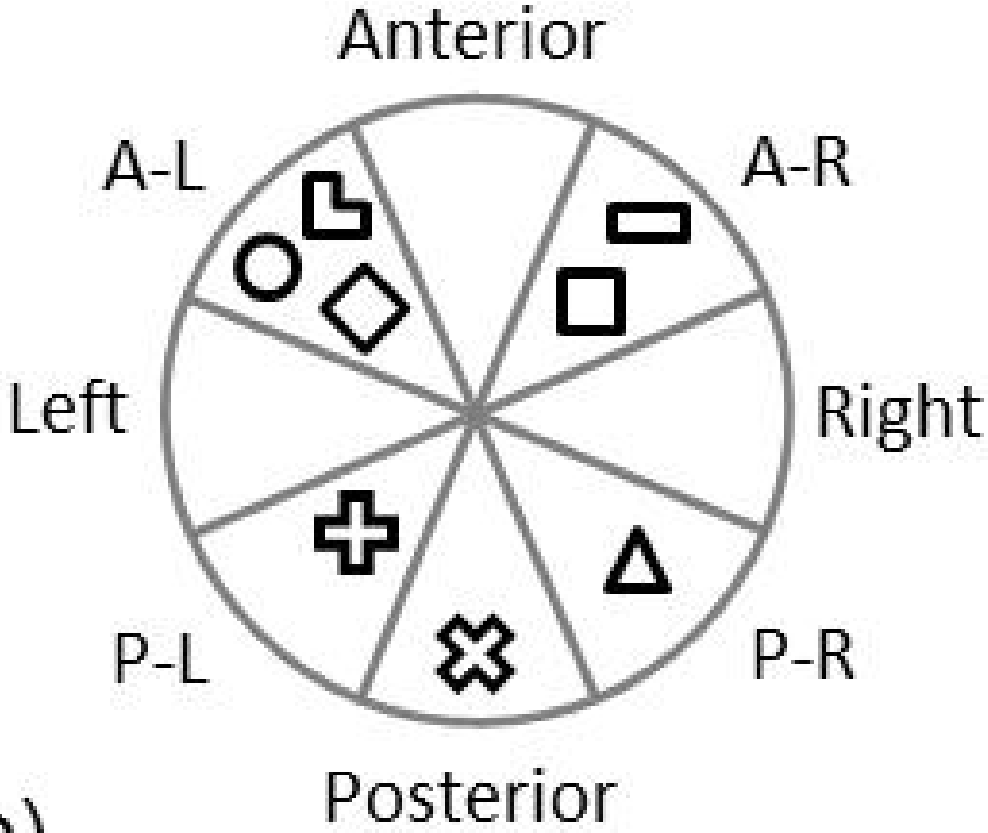
Anterior
A-L
A-R
Left
Right
P-L
P-R
Posterior

b)

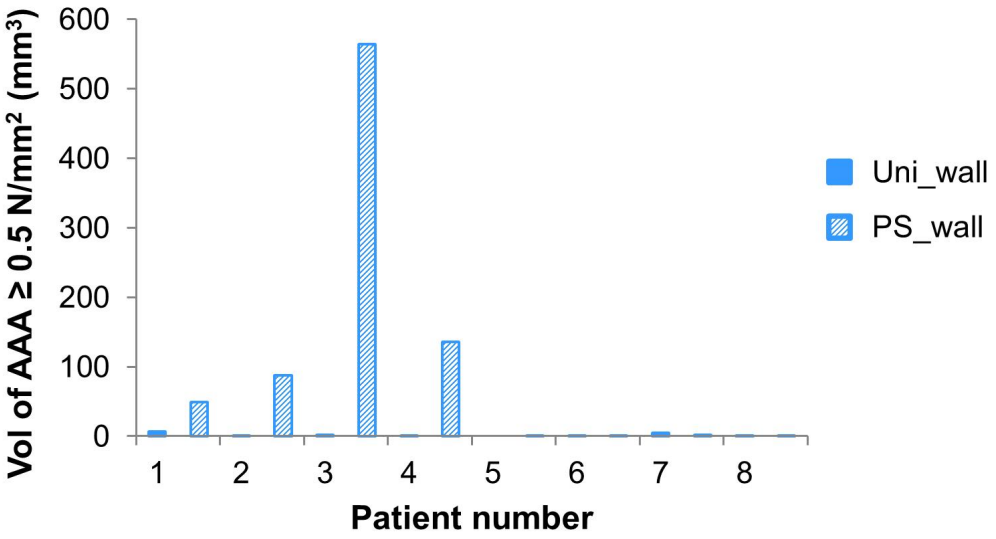
Vol of AAA ≥ 0.5 N/mm² (mm³)
600
500
400
300
200
100
0
1
2
3
4
5
6
7
8
Patient number
Uni_wall
PS_wall

a)

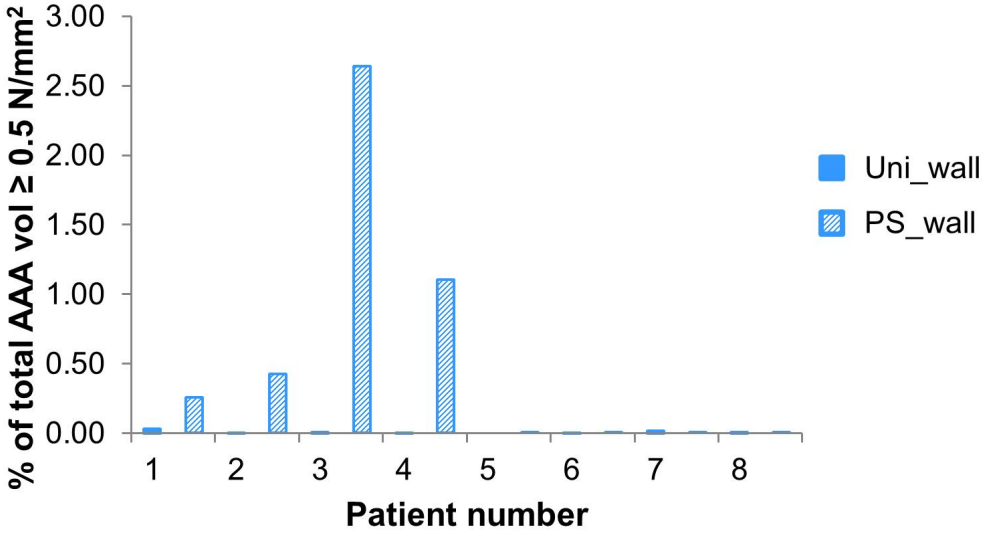
% of total AAA vol ≥ 0.5 N/mm²
3.00
2.50
2.00
1.50
1.00
0.50
0.00
1
2
3
4
5
6
7
8
Patient number
Uni_wall
PS_wall

b)

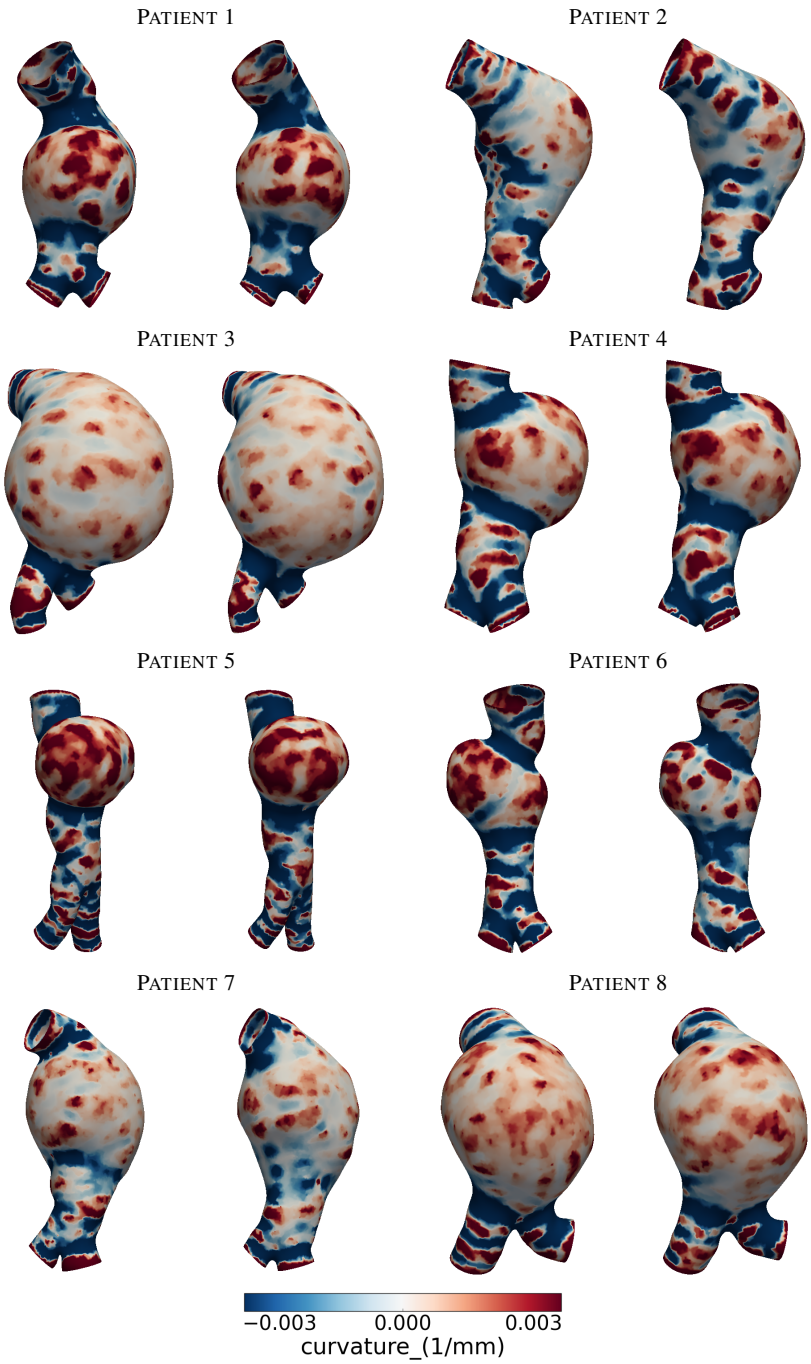
PATIENT 1
PATIENT 2
PATIENT 3
PATIENT 4
PATIENT 5
PATIENT 6
PATIENT 7
PATIENT 8
−0.003
0.000
0.003
curvature_(1/mm)

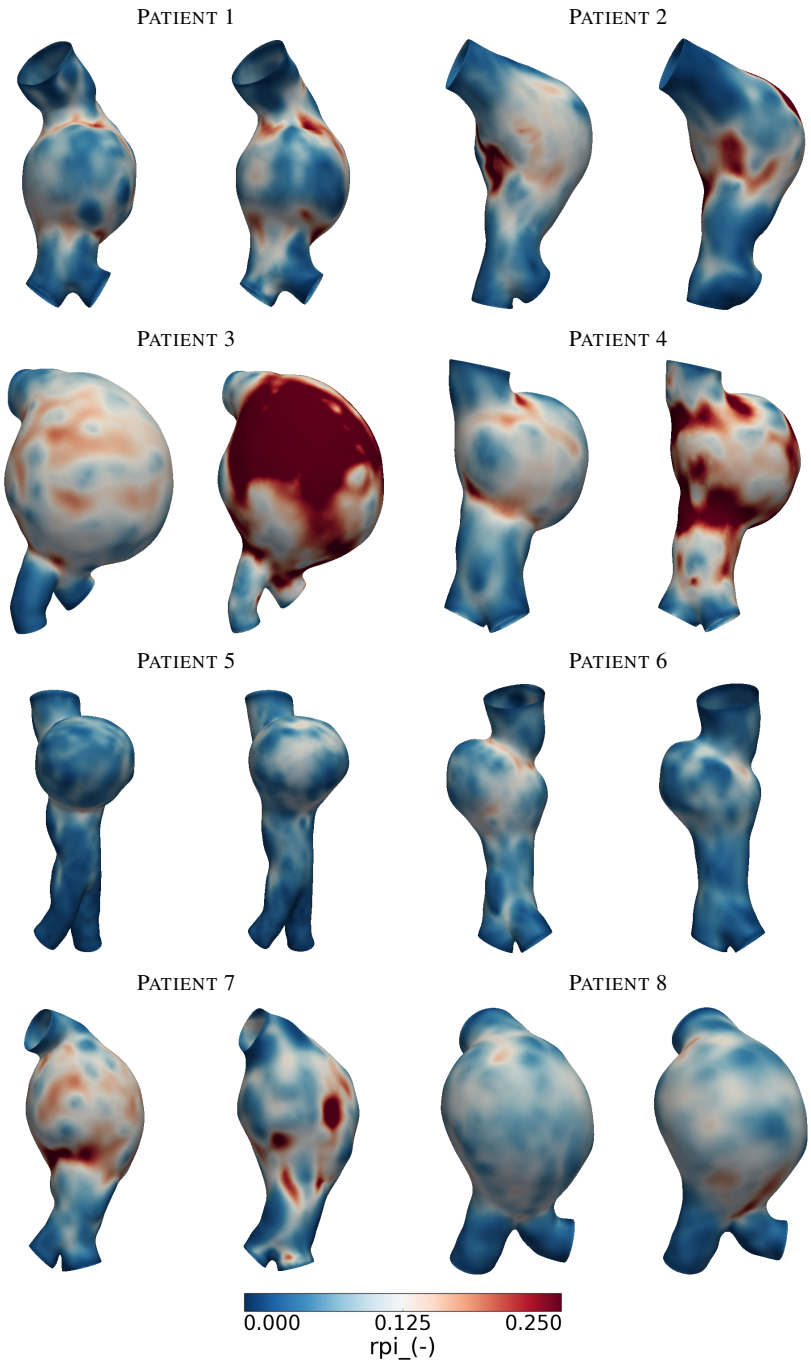
PATIENT 1
PATIENT 2
PATIENT 3
PATIENT 4
PATIENT 5
PATIENT 6
PATIENT 7
PATIENT 8
0.000
0.125
0.250
rpi_(-)

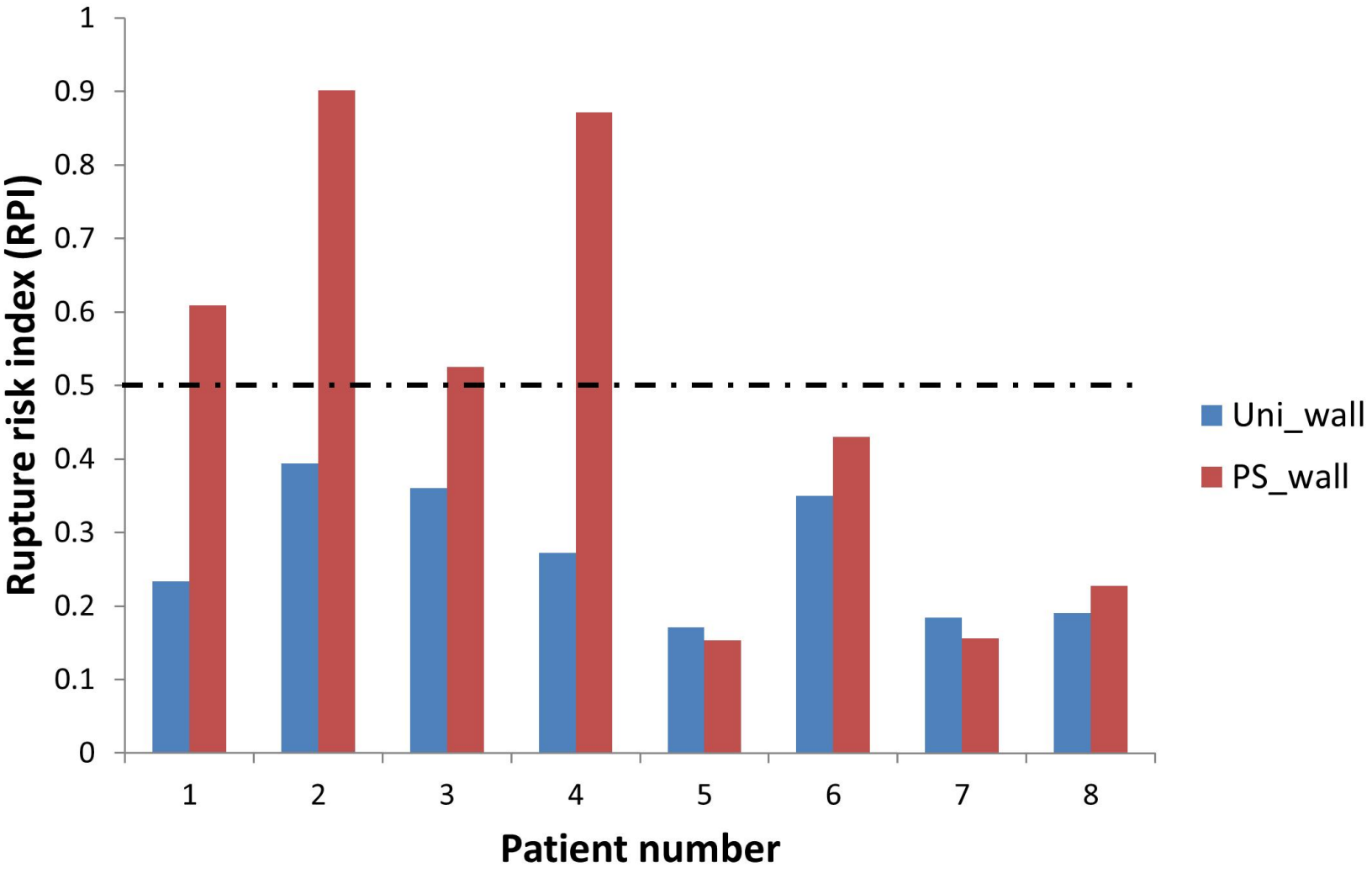
Rupture risk index (RPI)
1
0.9
0.8
0.7
0.6
0.5
0.4
0.3
0.2
0.1
0
1
2
3
4
5
6
7
8
Patient number
Uni_wall
PS_wall